Sensor and Simulation Notes

Note 425

19 August 1998

Selection of Angles Between Planes of TEM Feed Arms of an IRA

Carl E. Baum
Air Force Research Laboratory
Directed Energy Directorate

Abstract

Symmetry considerations have led to feed-arm structures for an impulse-radiating antenna lying on perpendicular planes (also perpendicular to the aperture plane). This paper extends these considerations to other constant-ϕ planes for the feed arms. Based on an approximation of this conductors of circular cross section, analytic formulae are obtained. Retaining horizontal and vertical symmetry planes, the position of the first feed-arm plane can be increased from a ϕ_0 of 45° (previous, noninteracting case) to somewhat larger values with some potential improvement in performance, depending on various factors. An interesting case has a ϕ_0 of 60° leading to a symmetrical 6-arm case with appropriate combinations of four arms giving various polarizations.

1. Introduction

In [2] various choices of feed-arm configurations for an impulse-radiating antenna (IRA) were discussed. Among these was a set of two arms of nominally 400Ω. There was also a set of four arms with one pair rotated by 90° with respect to the other so as not to interact significatnly with the other pair (by symmetry) giving a 200 Ω feed when appropriate arms are connected together. The arms can be circular cones or flat-plate cones, although the latter have the advantage that they can be oriented to minimize the aperture blockage in the case of a reflector IRA. Such feed structures have accurately calculable characteristic impedances, accomplished by a combination of stereographic and conformal transformations [4]. There it is also shown that, when appropriately used with a paraboloidal reflector, the spherical TEM wave on the feed exactly transforms to a planar TEM wave (before other scattering can reach the observer) according to the above stereographic transformation. This allows us to consider the two-dimensional form of the transmission-line feed in the calculations.

Summarizing from [3] we have the impulsive part of the far field on boresight as

$$\vec{E}_f(\vec{r},t) = \frac{V_0}{r}\frac{1}{2\pi c f_g}\vec{h}_a\,\delta_a\left(t-\frac{r}{c}\right)$$

$\delta_a \equiv$ approximate delta function $\rightarrow$ delta function as $r \rightarrow \infty$

$r =$ distance from aperture plane to observer

$t = 0 \equiv$ time step-function field arrives on antenna aperture δ_a

$f_g \equiv \frac{Z_c}{Z_0} = \frac{\Delta u}{\Delta v} \equiv$ geometrical impedance factor

$c \equiv$ speed of light $\simeq$ 2.997925 x 108 m/s

$\mu_0 \equiv 4\pi \times 10^{-7}$ H / m (1.1)

$Z_0 = \mu_0 c \simeq 376.73\ \Omega$

$\equiv$ wave impedance of free space

$V_0\,u(t) \equiv$ voltage on transmission-line at aperture plane

This leaves the equivalent height of the aperture

$$\vec{h}_a = h_{a_x}\vec{1}_x + h_{a_y}\vec{1}_y \tag{1.2}$$

which can be expressed in complex form as

$$h_a = h_{a_x} - jh_{a_y} = -\frac{1}{\Delta v} \oint_{C_a} v(\zeta) d\zeta^*$$

$$= \frac{j}{\Delta v} \oint_{C_a} u(\zeta) d\zeta^* \tag{1.3}$$

where

$$\begin{aligned} w(\zeta) \equiv u(\zeta) + jv(\zeta) &\equiv \text{ complex potential function} \\ \zeta \equiv x + jy &\equiv \text{ complex coordinate on aperture plane} \\ \Delta u &= \text{ change in the electric potential } u \text{ between conductors} \\ \Delta v &= \text{ change in the magnetic potnetial in going around conductors (say all the positive ones)} \\ C_a &\equiv \text{ aperture contour (boundary) with integral taken in positive direction (counter clockwise)} \end{aligned} \tag{1.4}$$

The form taken by the potential depends on the specific boundary value problem at hand. For present purposes, let us use a simple potential consisting of a linear combination of functions of the form

$$\begin{aligned} w &= -\ell n(\zeta - \zeta') \\ \zeta' &\equiv \text{ location of equivalent line charge} \end{aligned} \tag{1.5}$$

Here a minus sign corresponds to a positively charged wire; this reverses for a negatively charged wire. We constrain the sum of the wire charges to be zero to give a finite energy per unit length for differential TEM modes.

Figure 1.1 shows the general configuration of the aperture and feed. For convenience we define a parameter

$$\xi \equiv \frac{r_0}{a} \equiv \frac{\text{wire radius}}{\text{aperture radius}} \tag{1.6}$$

which we approximate as being small. The wire center is at a distance $a' > a$ from the origin which is clarified in the next section. In the cylindrial (Ψ, ϕ) coordinates given by

$$\begin{aligned} x &= \Psi \cos(\phi) \quad , \quad y = \Psi \sin(\phi) \\ \zeta &= \Psi e^{j\phi} \end{aligned} \tag{1.7}$$

the wires (circular cylinders) have centers on values of ϕ given by $\pm\phi_0$ and $\pm[\pi - \phi_0]$ with upper wires positive and lower wires negative.

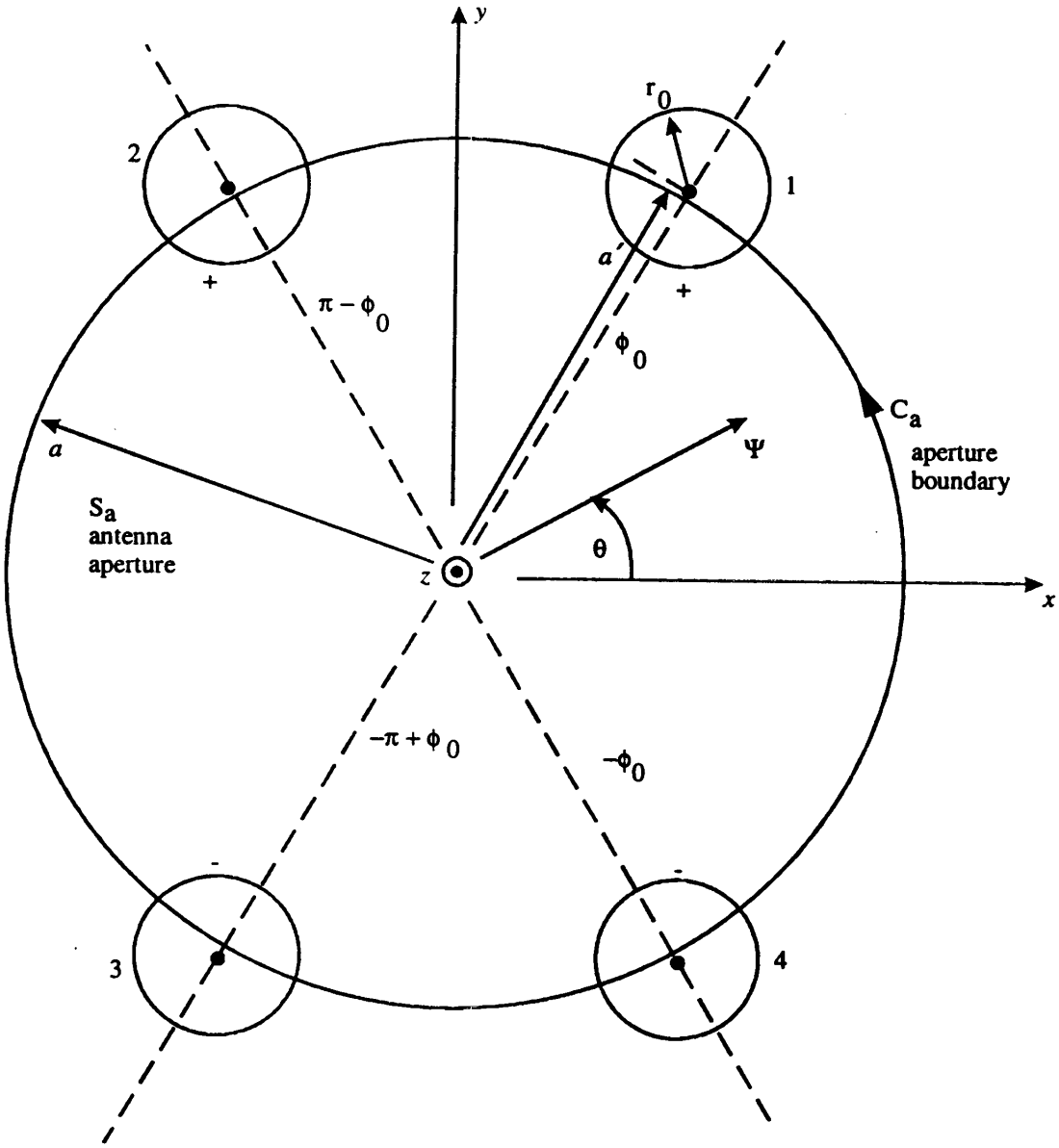

Fig. 1.1. Four-Wire TEM Transmission-Line Feed for Circular Aperture.

2. Two-Wire Feed

First we consider the case of a single two-wire feed (superscript 1) located at $\phi_0 = \pm\pi/2\,(90°)$. Summarizing from [3] we have

$$
\begin{aligned}
a'^2 &= a^2 + r_0^2 \\
w^{(1)}(\zeta) &= \ell n\left(\frac{\zeta + ja}{\zeta - ja}\right) \\
\Delta v^{(1)} &= 2\pi \\
\Delta u^{(1)} &= 2\ \operatorname{arccosh}\left(\frac{a'}{r_0}\right) = 2\ell n\left(\frac{a'}{r_0} + \left[\left[\frac{a'}{r_0}\right]^2 - 1\right]^{\frac{1}{2}}\right) \\
&= 2\ell n\left(\frac{a}{r_0} + \left[\left[\frac{a}{r_0}\right]^2 + 1\right]^{\frac{1}{2}}\right) = 2\ \operatorname{arcsinh}\left(\frac{a}{r_0}\right) \\
&= 2\ \operatorname{arcsinh}\left(\xi^{-1}\right) \\
&= 2\ell n\left(\frac{2}{\xi}\right) + O\left(\xi^2\right) \text{ as } \xi \to 0 \\
f_g^{(1)} &= \frac{1}{\pi}\ \operatorname{arcsinh}\left(\xi^{-1}\right) \\
&= \frac{1}{\pi}\ell n\left(\frac{2}{\xi}\right) + O\left(\xi^2\right) \\
\vec{h}_a^{(1)} &= h_{a_y}^{(1)}\,\vec{1}_y \\
h_{a_y}^{(1)} &= a\left[1 + O(\xi)\right] \text{ as } \xi \to 0 \\
\vec{h}_a^{(1)} &= -jh_{a_y}^{(1)} \simeq -ja
\end{aligned}
\tag{2.1}
$$

The two-wire case has an exact potential function as given above. Contours of constant u being circles, one of these is taken to define each wire. This in turn relates a' to a.

3. Four-Wire Feed

Now consider the case of a four-wire feed (superscript 2) with ϕ_0 general as in fig. 1.1. For evaluating $\vec{h}_a$ we can use symmetry. Define wire-pair 1 as wires 1 and 3. Consider this as a two-wire case as in Section 2, except that it is rotated by $-[\pi/2-\phi_0]$. Similarly define wire-pair 2 as wires 2 and 4. This is also like that in Section 2, except that it is rotated by $\pi/2-\phi_0$.

Write the equivalent height of the aperture in complex form as

$$h_a^{(2)} = \frac{1}{\Delta v^{(2)}}\left[j \oint_{C_a} u_1(\zeta) d\zeta^* + j \oint_{C_a} u_2(\zeta) d\zeta^* \right] \tag{3.1}$$

where the electric potential has been written as the sum of two terms, one associated with each of the wire pairs defined above (and identified by subscript). Now relate these electric potentials to the case in Section 2 via rotations as

$$\begin{aligned} j\oint_{C_a} u_1(\zeta) d\zeta^* &= j e^{j\left[\frac{\pi}{2}-\phi_0\right]} \oint_{C_a} u^{(1)}(\zeta) d\zeta^* \\ &= e^{j\left[\frac{\pi}{2}-\phi_0\right]} \Delta v^{(1)} h_a^{(1)} \\ j\oint_{C_a} u_2(\zeta) d\zeta^* &= j e^{-j\left[\frac{\pi}{2}-\phi_0\right]} \oint_{C_a} u^{(1)}(\zeta) d\zeta^* \\ &= e^{-j\left[\frac{\pi}{2}-\phi_0\right]} \Delta v^{(1)} h_a^{(1)} \end{aligned} \tag{3.2}$$

Here we have assumed that the presence of wire-pair 2 does not significatnly distort $u_1(\zeta)$ except in the vicinity of the (thin) wires (and conversely). Combining these gives

$$\begin{aligned} h_a^{(2)} &\simeq \cos\left(\frac{\pi}{2}-\phi_0\right) h_a^{(1)} = \sin(\phi_0)\, h_a^{(1)} \\ &= -j\, \sin(\phi_0) \end{aligned} \tag{3.3}$$

In vector form this is

$$\begin{aligned} &\vec{h}_a^{(2)} = \vec{h}_{a_y}^{(2)} \vec{1}_y \\ &\vec{h}_{a_y}^{(2)} \simeq \sin(\phi_0)\, a \end{aligned} \tag{3.4}$$

which is a rather simple result, valid for small ξ.

For the geometrical impedance factor we need to evaluate $\Delta u^{(2)}$. For this purpose, let us evaluate u_2 on wire 1. From the complex potential in (1.5) we have

$$\begin{aligned} w_2(\zeta) &= -\ell n\left(\zeta - a e^{j[\pi-\phi_0]}\right) + \ell n\left(\zeta - a e^{-j\phi_0}\right) \\ &= \ell n\left(\frac{\zeta - a e^{-j\phi_0}}{\zeta + a e^{-j\phi_0}}\right) \\ u_2(\zeta) &= \mathrm{Re}\left(w_2(\zeta)\right) = \ell n\left(\left|\frac{\zeta - a e^{-j\phi_0}}{\zeta + a e^{-j\phi_0}}\right|\right) \end{aligned} \tag{3.5}$$

Evaluating this on wire 1 let us take ζ as $e^{j\phi_0}$ since the associated electric field incident on wire 1 is approximately uniform there. By symmetry the associated part of $\Delta u^{(2)}$ is twice this value (counting contribution at wire 3). Adding the contribution from $u_1(\zeta)$ (wires 1 and 3 on themselves) as in (2.1) we have

$$\Delta u^{(2)} \simeq 2\left[\operatorname{arcsinh}\left(\xi^{-1}\right) + \ell n\left(\left|\frac{a' e^{j\phi_0} - a e^{-j\phi_0}}{a' e^{j\phi_0} + a e^{-j\phi_0}}\right|\right)\right] \tag{3.6}$$

Now approximating a' as nearly a form small ξ we have

$$\begin{aligned} \Delta u^{(2)} &\simeq 2\left[\operatorname{arcsinh}\left(\xi^{-1}\right) + \ell n\left(\tan(\phi_0)\right)\right] \\ f_g^{(2)} &= \frac{\Delta u^{(2)}}{\Delta v^{(2)}} \simeq \frac{1}{2\pi}\left[\operatorname{arcsinh}\left(\xi^{-1}\right) + \ell n\left(\tan(\phi_0)\right)\right] \\ &\simeq \frac{1}{2\pi}\left[\ell n\left(\frac{2}{\xi}\right) + \ell n\left(\tan(\phi_0)\right)\right] \text{ for small } \xi \\ &= \frac{1}{2\pi}\,\ell n\left(\frac{2\tan(\phi_0)}{\xi}\right) \end{aligned} \tag{3.7}$$

From (1.1) we have that the far field is proportional to

$$\frac{h_{a_y}^{(2)}}{f_g^{(2)}} = \mathrm{X}^{(2)}\, a$$
$$\mathrm{X}^{(2)} \simeq \frac{\sin(\phi_0)}{f_g^{(2)}} \simeq \frac{2\pi\sin(\phi_0)}{\ell n\left(\frac{2\tan(\phi_0)}{\xi}\right)} \tag{3.8}$$

This shows the influence of ϕ_0 and ξ together so that tradeoffs can be made. Also note that a realistic source does not rise in zero time, and the maximum rate of rise is a function of Z_c, and hence f_g.

A convenient value of Z_c is 200 Ω, being exactly four times 50Ω [2]. For the case of $\phi_0 = \pi/4$ (45°) this corresponds to 400Ω for a single pair of feed arms as in Section 2. For the four-wire feed we have

$$f_g^{(2)} = \frac{Z_c}{Z_0} \simeq 0.53088$$
$$2\pi f_g^{(2)} \simeq 3.3356 \tag{3.9}$$

If we keep $f_g^{(2)}$ fixed as we vary ϕ_0, then ξ will also vary. Consider then a few values of ϕ_0 in the following table.

Table 3.1. Parameters for 200 W Four-Wire Feed

ϕ_0	$\sin(\phi_0)$	$\tan(\phi_0)$	$\ell n(\tan(\phi_0))$	$\ell n\left(\frac{2}{\xi}\right)$	ξ	$\cos(\phi_0)$
$\frac{\pi}{4}$ (45°)	$\frac{1}{\sqrt{2}} \simeq 0.707$	1	0	3.3356	0.07118	$\frac{1}{\sqrt{2}} \simeq 0.707$
$\frac{\pi}{3}$ (60°)	$\frac{\sqrt{3}}{2} \simeq 0.866$	$\sqrt{3} \simeq 1.732$	0.5493	2.7663	0.12329	0.5
$\frac{5\pi}{12}$ (75°)	0.9659	$2+\sqrt{3} \simeq 3.732$	1.317	2.0187	0.26566	0.2586

Here we see ξ significantly increase as ϕ_0 is increased from 45° (no interaction between arm pairs). Noting the approximation of small ξ the formula is not valid as $\phi_0 \to \pi/2$ (or 90°) In particular we need to require that

$$\xi = \frac{r_0}{a} << \cos(\phi_0) = \frac{\text{half spacing between wire centers}}{a} \tag{3.10}$$

The last column in the table indicates that 60° may be appropriate, but that 75° is too large, at least for the assumed 200Ω feed impedance.

Noting that a conducting circular cylinder of radius r_0 is approximately equivalent to a conducting strip of width $4r_0$ [4], these results can also be applied to flat-plate feed structures. With the plates lying on planes of constant ϕ, the high-frequency (optical) blockage of the wave coming from a paraboloidal reflector (reflector IRA) is negligible [2]. This high-frequency lack of blockage carries over from the case of $\phi_0 = \pi/4$ (or 45°) to larger values of ϕ_0. However, for lower frequencies the blockage is greater due to the wider plates [5], as well as due to orientation of the second feed pair (2 and 4) such that the conductors are not completely perpendicular to the electric field from the first feed pair (1 and 3) and conversely.

4. Six-Plate Feed

One application of the previous results is to a six-plate feed as in fig. 4.1. Utilizing the symmetry of the configuration in fig. 1.1, in which the electric field is perpendicular to the $y = 0$ plane, we can place another pair of feed arms (flat plates) on this plane with zero electric potential. For this configuration the case of $\phi_0 = \pi/3$ (or 60°) is particularly interesting due to the symmetry. This gives a 6-fold rotation axis with axial symmetry planes or C_{6a} symmetry [7]. In fig. 4.1, the polarization is vertical. However, by rotating the +, −, and 0 electric-potential labels in increments of 60° the polarization is similarly rotated with precisely the same antenna performance.

It is interesting to note that this special ϕ_0 of 60° (leading to the symmetrical 6-arm configuration) is also the special case for a 4-wire transmission line producing a uniform field (first three derivatives zero) at the center (i.e., (x, y) = (0, 0)) [1, 6].

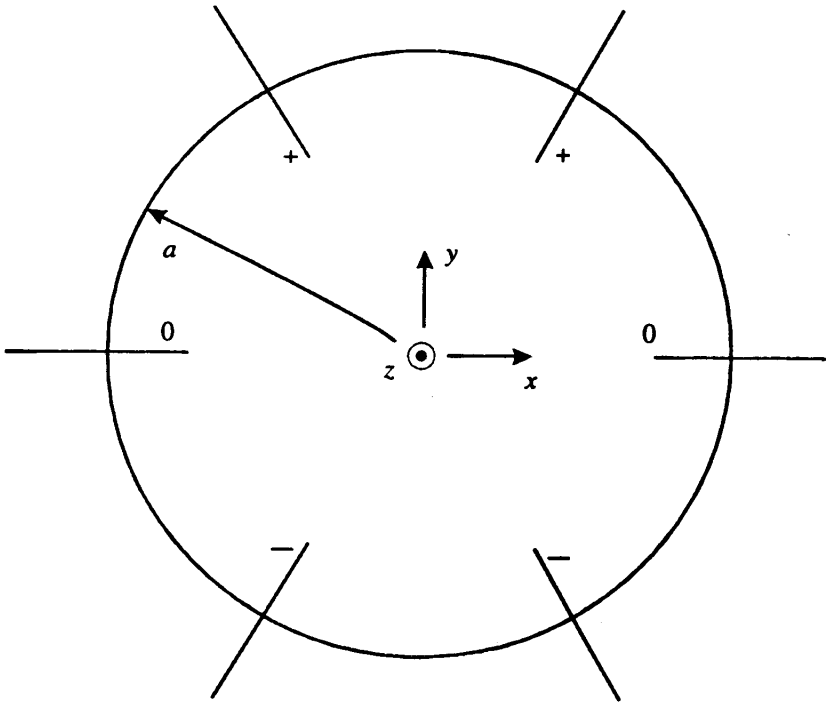

A. Aperture configuration

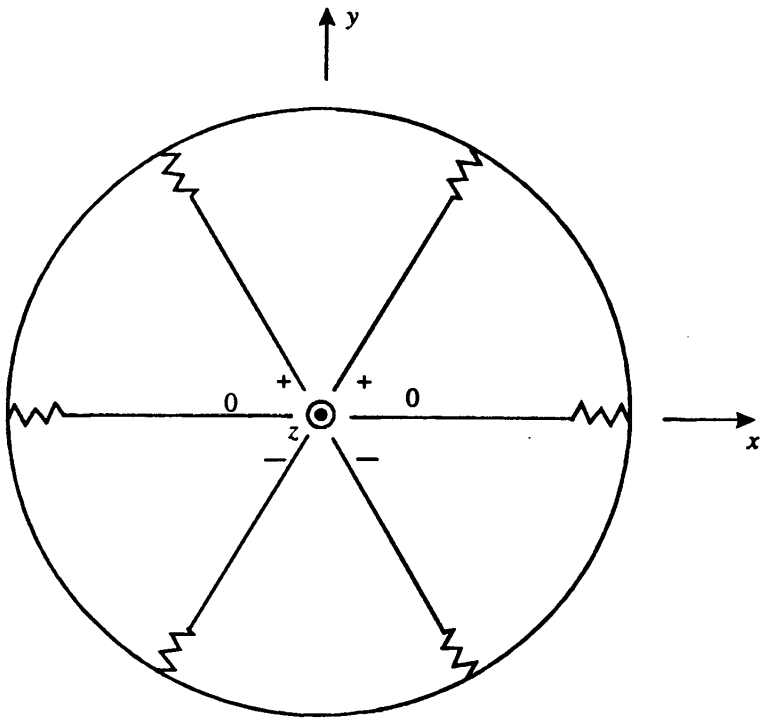

B. Reflector-IRA configuration

Fig. 4.1. Six-Plate Feed for an IRA; $\phi_0 = \pi/3$.

5. Concluding Remarks

This paper has begun some calculations for IRA feed plates on nonorthogonal planes. Since these are based on conductors of small circular cross section they can only be applied in an approximate way to more realistic configurations involving flat-plate feeds. Since there may be some benefits to choosing a more optimal angle between the constant-ϕ planes defining feed-conductor locations, more detailed calculations and canonical experiments may be in order.

References

1. C. E. Baum, Impedances and Field Distributions for Symmetrical Two Wire and Four Wire Transmission Line Simulators, Sensor and Simulation Note 27, October 1966.

2. C. E. Baum, Configurations of TEM Feed for an IRA, Sensor and Simulation Note 327, April 1991,

3. C. E. Baum, Aperture Efficiencies for IRAs, Sensor and Simulation Note 328, June 1991.

4. E. G. Farr and C. E. Baum, Prepulse Associated with the TEM Feed of an Impulse Radiating Antenna, Sensor and Simulation Note 337, March 1992.

5. D. V. Giri and C. E. Baum, Reflector IRA Design and Boresight Temporal Waveforms, Sensor and Simulation Note 365, February 1994.

6. C. E. Baum, Two-Dimensional Coils for Low-Frequency Magnetic Illumination and Detection, Sensor and Simulation Note 406, November 1996.

7. C. E. Baum and H. N. Kritikos, Symmetry in Electromagnetics, ch. 1, pp. 1–90, in C. E. Baum and N. H. Kritikos (eds.), *Electromagnetic Symmetry*, Taylor & Francis, 1995.